Fluid Phase Equilibria 462 (2018) 172–180

Contents lists available at ScienceDirect

Fluid Phase Equilibria

journal homepage: www.elsevier.com/locate/fluid

Extractive distillation of methylal/methanol mixture using ethylene glycol as entrainer

Yichun Dong, Chengna Dai, Zhigang Lei*

State Key Laboratory of Chemical Resource Engineering, Beijing Key Laboratory of Energy Environmental Catalysis, Beijing University of Chemical Technology, Box 266, Beijing, 100029, China

ARTICLE INFO

Article history:
Received 10 November 2017
Received in revised form
30 January 2018
Accepted 31 January 2018
Available online 5 February 2018

Keywords:
Methylal
Methanol
Ethylene glycol
Extractive distillation
UNIFAC model
COSMO-RS model

ABSTRACT

Ethylene glycol (EG) is proposed as an entrainer for the separation of methylal and methanol by extractive distillation. The COSMO-RS model was used to screen the suitable entrainer in terms of selectivity and solvent capacity. EG is a suitable entrainer with a low environmental impact. Vapor −liquid equilibrium (VLE) experiments demonstrated that the relative volatility of methylal to methanol is significantly improved using EG as an entrainer. The new corresponding interaction parameters were obtained by correlating the VLE data using the UNIFAC model, and then they were introduced into the process simulation software. The extractive distillation process was simulated using the rigorous equilibrium stage model. The optimal operating conditions were obtained by sensitivity analysis. The simulation results showed that EG is effective and efficient for the separation of methylal and methanol. In addition, the COSMO-RS model provides some theoretical insights into the separation mechanism.

1. Introduction

Extractive distillation is commonly applied to separate azeotropes or close-boiling mixtures that can't be separated by conventional distillation because the relative volatility is approximately 1. In extractive distillation, an additional component (a salt solution or a solvent) is added to the mixture as an entrainer to increase the relative volatility. Because the affinity between the entrainer and the heavy key component is higher than that between the entrainer and the light key component, the light key component and heavy key component can be obtained at the top and the bottom of distillation column, respectively [1–4].

Methylal, also called dimethoxymethane, is an important intermediate and is widely used in many products (e.g., cosmetics, medicines, household goods, car polish, diesel fuel additive, and pesticides) [5–7]. Methylal is normally synthesized by the catalytic reaction of methanol and formaldehyde or paraformaldehyde. Because it is a reversible reaction, the production of methylal is restricted by chemical equilibrium [8]. Methylal and methanol form a minimum-boiling azeotropic mixture. Thus, extractive distillation is a possible way to separate the methylal and methanol azeotropic mixture.

In extractive distillation processes, the most important step is to choose an effective and economic entrainer. The entrainer must have special characteristics (e.g., low toxicity, easy recovery, thermal stability, high boiling point, high relative volatility between key components, and high solvent capacity) to achieve the desired separation [9]. Currently, four types of entrainers (i.e., liquid solvents [10], solid salts [11], hyperbranched polymers [12], and ionic liquids (ILs) [13]) have been used. The separation of methylal and methanol using different entrainers has been investigated by several researchers. For example, Liu et al. [14] investigated the integrated extractive catalytic distillation process using water as an entrainer and operating continuously with 98.0% formaldehyde conversion, and 98.7 wt% methylal was obtained. However, some water was contained in the product. Wang et al. [15] investigated the separation of methylal and methanol using dimethylformamide (DMF) as an entrainer by extractive distillation. A high purity of methylal was obtained, but DMF isn't an environment friendly solvent. To intensify the separation of methylal and methanol, it is necessary to identify a new entrainer.

The separation process is designed and analyzed after an appropriate entrainer is chosen. The most important step is to understand the behavior of the mixture according to its appropriate trajectory including liquid-liquid, vapor-liquid, or vapor-liquid-

* Corresponding author.
E-mail address: leizhg@mail.buct.edu.cn (Z. Lei).

https://doi.org/10.1016/j.fluid.2018.01.038
0378-3812/

liquid equilibrium [16]. The residue curve maps (RCMs) are crucial graphical tools for vapor-liquid separations in extractive distillation processes [17,18]. In the RCM, the pure solvent composition and the minimum-boiling azeotropic point are a stable node and an unstable node, respectively. Thus, there are no distillation boundaries in the diagram and all the components can be obtained as pure products [19].

The content of this work is organized as follows. First, the potential entrainers were screened by considering both selectivity and solvent capacity as predicted by the COSMO-RS model using the COSMOthermX package (version C30_1301). Second, the vapor-liquid equilibrium (VLE) for the methylal-methanol-ethylene glycol (EG) system was measured at 101.3 kPa, and the application of the UNFAC model was extended based on the VLE data. Third, we tried to seek for some theoretical insights at the molecular level to explain the separation mechanism. Finally, the rigorous equilibrium (EQ) stage model of the extractive distillation process was established by inputting the corresponding UNFAC model parameters into the process simulation software (Aspen Plus 8.4). Thus, this work ranges from the molecular level to a systematic scale.

2. Experimental

2.1. Materials

The experimental materials used in this work were methylal, methanol, and EG. Methylal with a purity above 98 wt% was obtained from Shanghai Aladdin Biological Technology Co. Ltd. Methanol with a purity above 99.9 wt% was supplied by Beijing MREDA Scientific Ltd. EG with a purity above 99.5 wt% was supplied by Tianjin Guangfu Fine Chemical Research Institute. No significant impurities were identified in any of the reagents based on chromatographic analysis. A Karl Fischer titration (KLS701) was used to measure the water content, and the results showed a water content below 1000 ppm in the pure organic components. Consequently, no purification methods were applied. The chemical properties of the materials used in this work are listed in Table 1.

2.2. Apparatus and procedure

The VLE data for the methylal + methanol + EG ternary system were measured in a circulation VLE still (a modified Othmer still) at atmospheric pressure. The details of this apparatus can be found in our previous works [20–22]. The compositions of methylal, methanol, and EG in the vapor and liquid phases were analyzed using gas chromatography (GC 4000A) equipped with a flame ionization detector (FID) and HJ-WAX column (60 m × 0.32 mm). The estimated uncertainties in temperature and mole fractions in the vapor and liquid phases are $u(T)$, $u(x)$, and $u(y)$, respectively. The values of $u(T)$, $u(x_1)$, and $u(y_1)$ in the binary system are 0.11 K, 0.007, and 0.008, respectively. The values of $u(T)$, $u(x_i)$, and u(y_i) in the ternary system are 0.12 K, 0.007, and 0.007, respectively.

3. Computational section

3.1. UNIFAC model

The UNIFAC model, based on group contribution method, was used to calculate the activity coefficients at infinite dilution and finite concentrations. The UNIFAC model can be used to predict the thermodynamic properties of systems that lack experimental data and contain basic groups based on limited group characteristic parameters.

In this work, the UNIFAC model was applied to describe the thermodynamic phase equilibrium relevant to the separation of methylal and methanol, in which the methylal, methanol, and EG molecules were each regarded as a separate group [23,24].

The activity coefficient is dependent on temperature and composition, and can be expressed as

$$\ln \gamma_i = \ln \gamma_i^{\mathrm{C}} + \ln \gamma_i^{\mathrm{R}} \tag{1}$$

where $\ln \gamma_i^C$ represents the combinatorial contribution to the activity coefficient from the difference in size and shape of different groups and $\ln \gamma_i^R$ represents the residual contribution to the activity coefficient from the interaction between different functional groups. The group binary interaction parameters, α_{mn} and α_{nm}, are contained within $\ln \gamma_i^R$. For the methylal-methanol-EG ternary system, the interaction parameters between the methylal and methanol groups [23], as well as those between methanol and EG, are available from previous publications [24]. However, the interaction parameters of methylal and EG groups are still vacant, and thus should be obtained by correlating the VLE data as measured in this work. The minimized average relative deviation (ARD) was used as the objective function (OF):

$$OF = \min\left\{\frac{1}{2N}\sum_{i=1}^{2}\sum_{j=1}^{N}\left|\frac{\gamma_{ij,cal}-\gamma_{ij,\exp}}{\gamma_{ij,exp}}\right|\right\} \tag{2}$$

where $\gamma_{ij,exp}$ and $\gamma_{ij,cal}$ represent the experimental and calculated activity coefficients, respectively, of component i at data point j in the liquid phase. N is the number of data points, which includes the activity coefficients of methylal and methanol used for data correlation.

$\gamma_{i,exp}$ was calculated from

$$\gamma_{i,\exp} = \frac{Py_i}{P_i^s x_i} \tag{3}$$

where P is the atmospheric pressure, x_i and y_i represent the mole fractions of component i in the liquid and vapor phases, respectively, and P_i^s is the vapor pressure of pure component i as calculated by the Antoine equation; the parameters of the Antoine equation [25,26] are listed in Table 2. All the group interaction parameters used in this work are listed in Tables 3 and 4.

Table 1
Chemical properties of the materials.

Material	CAS RN	Source	Mass fraction purity	Purification method	Analysis method
Methylal	109-87-5	Aladdin	≥98%	None	Gas chromatography
Methanol	67-56-1	MREDA	≥99.9%	None	Gas chromatography
Ethylene glycol	107-21-1	Tianjin Guangfu	≥99.5%	None	Gas chromatography

Table 2
Antoine coefficients A, B, and C.

Components	*A*	*B*	*C*	*T* range/K	Reference
Methylal[a]	14.2473	−2640.84	−41.22	273–357	[25]
Methanol[a]	16.5725	−3626.55	−34.29	257–364	[25]
EG[b]	4.97012	1914.951	−84.996	323–473	[26]

[a] $\ln(P^s/\text{kPa}) = A + B/[(T/\text{K}) + C]$.
[b] $\log_{10}(P^s/\text{bar}) = A - B/[(T/\text{K}) + C]$.

Table 3
UNIFAC group volume (R_k) and surface area (Q_k).

Group	R_k	Q_k
Methylal	2.9644	2.716
Methanol	1.4311	1.432
EG	2.4088	2.248

Table 4
The group interaction parameters of methylal, methanol, and EG in the UNIFAC model.

m	*n*	α_{mn}/K	α_{nm}/K
Methylal	Methanol	410.00	−71.21
Methylal	EG	445.38	−31.86
Methanol	EG	−119.2	240.8

3.2. COSMO-RS model

The COSMO-RS model was developed from COSMO (conductor-like screening model), in which the molecules around the solute are assumed to be electrical conductors, and the geometries of the solute molecules and the density of screening charge density (σ) on the surface of the solute molecules can be calculated using quantum chemical calculations [27,28]. In the COSMO-RS model, the surfaces of solute and solvent molecules are divided into many segments; thus, the discrete surfaces on the segments are characterized by their geometries and screening charge density (σ) at a minimum conductor energetic state. The complete interactions between the molecules are described by the screening charge density (σ) distribution σ-profiles $P_s(\sigma)$ [29]. Moreover, the screening charge converts the molecular polarity information into standard thermodynamic data [30,31].

The COSMO-RS model has been used to predict the thermodynamic properties and phase behavior of pure components and mixtures [27,28,32–36]. The COSMOthermX software (version C30_1301), based on the COSMO-RS model, was applied to screen the suitable entrainer for extractive distillation and to analyze the σ-profiles and σ-potentials of the pure components investigated in this work. It contains a large databank that includes many common geometries; however, many unusual molecules are not included. To calculate the thermodynamic properties, the new molecules must be first optimized using quantum mechanical (QM) software (e.g., DMol3, HyperChem, TURBOMOLE, MOPAC, and Gaussian), and then introduced into the software.

In this work, methanol and EG were obtained from the TZVP-C30–1301 databank, whereas methylal, DMF, ethanolamine, sulfolane, and *N*-methyl-2-pyrrolidinone (NMP) were first optimized using the Gaussian 09 package to generate the COSMO files, which were then introduced into the COSMOthermX package. Then, the thermodynamic properties were computed for the pure components or mixtures. The polarization charge densities (σ-profiles) and the affinity of the molecule for surface of polarity σ (σ-potentials) for methanol, methylal and EG were analyzed using the COSMO-RS model, thus providing some theoretical insights into the methylal and methanol separation at a molecular level.

3.3. Process simulation

The extractive distillation process for the separation of methylal and methanol using EG as an entrainer was simulated using the Aspen Plus software (version 8.4) with the RadFrac rigorous EQ stage model [37–40]. The new UNIFAC model parameters were input into the EQ stage model. During the process simulation, methanol, methylal, and EG were considered conventional compounds by default.

4. Results and discussion

4.1. Screening of entrainers for the separation of methylal and methanol

The selectivity and solvent capacity are crucial for screening the most suitable entrainer. The selectivity (S) can be expressed as

$$S_{12}^{\infty} = \frac{\gamma_1^{\infty}}{\gamma_2^{\infty}} \tag{4}$$

where γ_i^{∞} represents the activity coefficient of component i at infinite dilution.

The solvent capacity (SP) is expressed as

$$SP = \frac{1}{\gamma_1^{\infty}} \tag{5}$$

A suitable entrainer should have both high selectivity and high solvent capacity. In extractive distillation, the solvent capacities of both the light and heavy components are important because immiscibility could reduce the separation factor. In this work, methanol itself is a very good solvent which is miscible with entrainer. Thus, the solvent capacity of methanol wasn't considered, and we only need to consider the solvent capacity of methylal. For pre-selection, the suitable entrainer was screened by the COSMO-RS model in terms of selectivity and solvent capacity at infinite dilution at 298.15 K. As shown in Fig. 1, the selectivity of methylal to methanol follows the trend of DMF > NMP > EG > ethanolamine > sulfolane, while the solvent capacity follows the trend of ethanolamine > EG > NMP > DMF > sulfolane. This means that an entrainer with a higher selectivity doesn't always possess a higher capacity. Among these entrainers, EG has an appropriate selectivity and solvent capacity. Moreover, EG was selected as a suitable entrainer

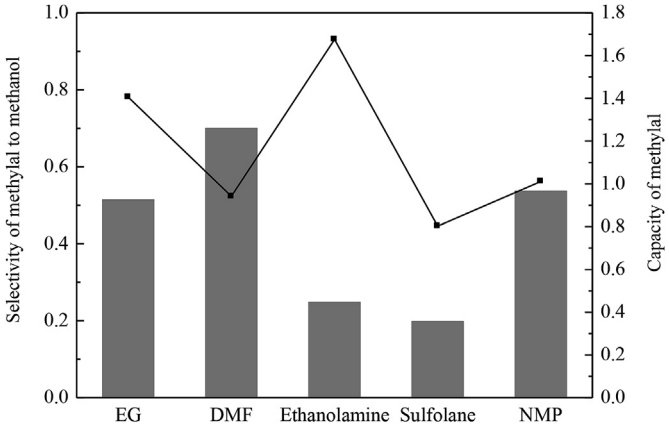

Fig. 1. Selectivity of methylal to methanol and solvent capacity of methylal at infinite dilution calculated using the COSMO-RS model at $T = 298.15$ K (bar, selectivity; line, solvent capacity).

for the separation of methylal and methanol because it has a low toxicity and low vapor pressure, and it is inexpensive.

4.2. Residue curve maps

RCMs describe the system composition in the liquid phase during a batch variation distillation; RCMs are often used to design and analyze the distillation process, including extractive distillation processes.

In general, the RCMs of azeotropic systems are divided into different distillation regions. However, only one distillation region exists in the RCM investigated in this work. Fig. 2 shows the RCM for the methylal (1) + methanol (2) + EG (3) ternary system as calculated by the UNIFAC model. The direction of the residual curves points from an unstable node (the binary azeotrope of methylal and methanol) to a stable node (EG) as the distillation time increases. The rest of the vertices that correspond to pure components are saddle points. The red dashed line plotted in Fig. 2 is the isovolatility line [41], in which all points in the presence of the entrainer have a relative volatility of methylal to methanol equal to 1. The isovolatility line divides the RCM into two regions. In region I, the local volatility follows the trend of methanol > methylal > EG, while in region II, the local volatility follows the trend of methylal > methanol > EG. In region I, methanol is the most volatile component, while in region II, methylal is the most volatile component. Moreover, region II is significantly larger than region I, indicating that EG is an appropriate entrainer for the separation of methylal and methanol. If the isovolatility line intersects the methylal–EG edge, the more volatile component (methylal) in the mixture can be obtained at the top of the extractive distillation column. Evidently, this provides a guide to design of the extractive distillation process [41].

4.3. Relative volatility using EG as an entrainer

The measured VLE data for the binary system of methylal + methanol are listed in Table 5. The thermodynamic consistency of the binary VLE data is validated to test the reliability of the experimental data [42]. The plot of $\ln(\gamma_1/\gamma_2)$ - x_1 is illustrated in Fig. 3, and it provides the following results: $D = 0.18$ and $J = 6.87$. Thus, the value of $D - J$ is −6.69 (which is < 10), indicating that the experimental data measured in this work satisfy the thermodynamic consistency test.

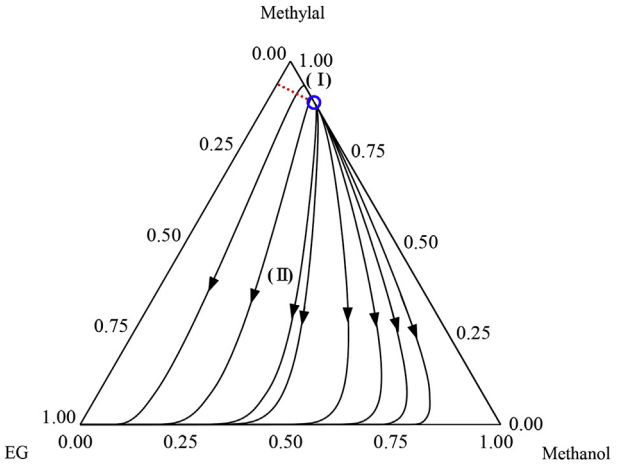

Fig. 2. RCM for the ternary system of methylal + methanol + EG at 101.3 kPa (red dashed line, isovolatility line; ○, azeotropic point). (For interpretation of the references to colour in this figure legend, the reader is referred to the Web version of this article.)

Table 5
VLE data for methylal (1) + methanol (2) at 101.3 kPa.

T (K)	x_1	y_1	P_1^S (kPa)	P_2^S (kPa)	γ_1	γ_2
329.41	0.0978	0.4005	161.36	72.45	2.5723	0.9293
323.20	0.2123	0.5891	131.89	55.66	2.1321	0.9495
320.67	0.2961	0.6664	121.17	49.83	1.8819	0.9638
317.77	0.4457	0.7314	109.72	43.77	1.5156	1.1215
316.33	0.5951	0.7812	104.38	41.01	1.2742	1.3354
315.29	0.7462	0.8261	100.66	39.12	1.1145	1.7744
315.11	0.8461	0.8704	100.01	38.79	1.0422	2.1995
315.09	0.8980	0.8991	99.94	38.75	1.0151	2.5864
315.59	0.9498	0.9417	101.70	39.65	0.9877	2.9698

Standard uncertainties u are: $u(T) = \pm 0.11$ K, $u(x_1) = \pm 0.007$, and $u(y_1) = \pm 0.008$.

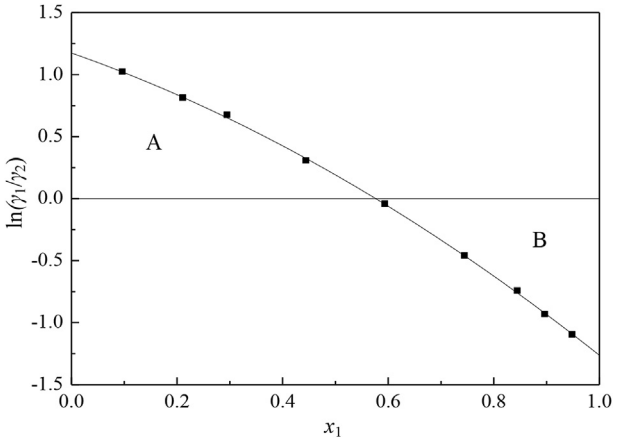

Fig. 3. Thermodynamic consistency test.

On this basis, the VLE experimental data for the methylal (1) + methanol (2) + EG (3) ternary system is listed in Table 6. The relative volatility (α_{12}) of methylal (1) to methanol (2) was calculated by

$$\alpha_{12} = \frac{y_1/x_1}{y_2/x_2} \tag{6}$$

where x_i and y_i represent the mole fractions of component i in the liquid and vapor phases, respectively.

The x_1'-y_1' (on an entrainer-free basis) and x_1'-α_{12} plots, are shown in Figs. 4 and 5, respectively, with the predicted results using the UNIFAC model. With the increase in the EG content, the relative volatility of methylal to methanol significantly increases, indicating that EG is a suitable entrainer for the separation of methylal and methanol. Moreover, the UNIFAC predictions and experimental data agree. The ARD for the methylal-methanol-EG ternary system is only 5.28%, confirming the prediction accuracy of the UNIFAC model. This means that the new UNIFAC parameters can be further input into the commercial process simulation software (e.g., Aspen Plus, PROII, etc.) for the simulation and optimization of the extractive distillation processes.

4.4. Analysis of the σ-profiles and σ-potentials

The σ-profiles and σ-potentials obtained from the COSMO-RS model were applied to analyze the separation mechanism of the methylal-methanol-EG system at a molecular level [29,43,44]. σ-Profiles, a crucial parameter in the COSMO-RS model, represent the distribution of the screening charge density (σ) on the surface of molecule, while the σ-potentials reveal the affinity of a molecule toward a surface of polarity σ. The σ-profile consists of three parts:

Table 6
VLE experimental data and UNIFAC predicted values for methylal (1) + methanol (2) + EG (3) at 101.3 kPa.

T/K	Liquid phase		Vapor phase				$\gamma_{1,exp}$	$\gamma_{2,exp}$	$\gamma_{1,cal}$	$\gamma_{2,cal}$	RD1	RD2
	x_1	x_2	$y_{1,exp}$	$y_{2,exp}$	$y_{1,cal}$	$y_{2,cal}$						
316.15	0.5735	0.0320	0.9722	0.0273	0.9832	0.0164	1.6125	2.1016	1.6316	1.2619	0.0118	0.3996
317.04	0.5133	0.0928	0.9562	0.0433	0.9535	0.0462	1.7179	1.1035	1.7436	1.1992	0.0149	0.0868
317.45	0.4529	0.1526	0.9319	0.0675	0.9251	0.0746	1.8683	1.0259	1.8774	1.1480	0.0048	0.1190
318.56	0.3608	0.2468	0.8850	0.1144	0.8776	0.1220	2.1410	1.0217	2.1192	1.0882	0.0102	0.0651
321.36	0.2713	0.3368	0.8416	0.1576	0.8192	0.1804	2.4582	0.9103	2.4108	1.0498	0.0193	0.1532
325.45	0.1820	0.4267	0.7637	0.2353	0.7299	0.2696	2.9010	0.8982	2.7687	1.0282	0.0456	0.1447
331.05	0.1220	0.4883	0.6581	0.3403	0.6236	0.3758	3.1120	0.8975	3.0421	1.0223	0.0224	0.1391
339.60	0.0609	0.5479	0.4455	0.5517	0.4289	0.5701	3.2378	0.9197	3.3575	1.0236	0.0370	0.1130
316.94	0.7629	0.0415	0.9738	0.0257	0.9716	0.0281	1.1807	1.4725	1.1927	1.6304	0.0101	0.1072
316.80	0.6789	0.1252	0.9246	0.0749	0.9246	0.0752	1.2626	1.4261	1.2808	1.4530	0.0144	0.0189
317.05	0.6000	0.2034	0.8818	0.1177	0.8878	0.1121	1.3545	1.3681	1.3847	1.3227	0.0223	0.0332
317.63	0.4803	0.3244	0.8323	0.1671	0.8354	0.1645	1.5609	1.1833	1.5868	1.1794	0.0166	0.0033
319.25	0.3594	0.4455	0.7703	0.2291	0.7764	0.2235	1.8246	1.0978	1.8619	1.0843	0.0204	0.0123
323.21	0.2398	0.5654	0.6936	0.3056	0.6880	0.3119	2.1501	0.9682	2.2201	1.0285	0.0325	0.0623
326.90	0.1593	0.6459	0.6099	0.3890	0.5891	0.4107	2.5279	0.9242	2.5237	1.0086	0.0017	0.0913
333.45	0.0799	0.7254	0.4167	0.5815	0.4085	0.5912	2.7907	0.9368	2.8768	1.0015	0.0309	0.0691
316.70	0.6669	0.0366	0.9783	0.0212	0.9787	0.0209	1.3623	1.3855	1.3821	1.3855	0.0145	0.0000
316.96	0.5961	0.1092	0.9405	0.0589	0.9414	0.0583	1.4524	1.2751	1.4816	1.2862	0.0201	0.0087
317.17	0.5297	0.1772	0.9093	0.0902	0.9095	0.0902	1.5690	1.1922	1.5934	1.2103	0.0156	0.0152
318.08	0.4207	0.2848	0.8608	0.1387	0.8597	0.1401	1.8121	1.0945	1.8273	1.1162	0.0084	0.0198
319.96	0.3138	0.3921	0.8071	0.1922	0.8001	0.1997	2.1349	1.0130	2.1218	1.0553	0.0062	0.0417
324.11	0.2098	0.4975	0.7137	0.2854	0.7099	0.2898	2.4642	0.9923	2.4834	1.0210	0.0078	0.0289
328.56	0.1396	0.5671	0.6293	0.3694	0.6076	0.3920	2.8212	0.9325	2.7813	1.0102	0.0141	0.0833
336.10	0.0705	0.6365	0.4253	0.5725	0.4210	0.5783	2.9824	0.9465	3.1148	1.0085	0.0444	0.0656
										ARD =	0.0528	

Standard uncertainties u are: $u(T) = \pm 0.12$ K, $u(x_i) = \pm 0.007$, and $u(y_i) = \pm 0.007$.

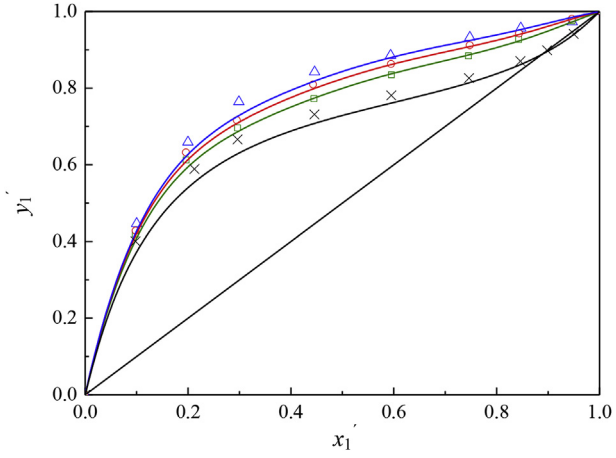

Fig. 4. Isobaric VLE data for the methylal (1) + methanol (2) + EG (3) system at 101.3 kPa (lines, predicted data by the UNIFAC model; scattered points, experimental data; ×, $x_3 = 0$; □, $x_3 = 20\%$; ○, $x_3 = 30\%$; △, $x_3 = 40\%$).

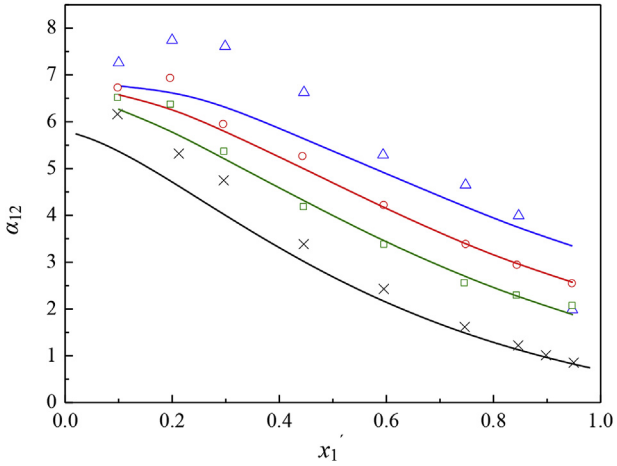

Fig. 5. Relative volatility of methylal (1) to methanol (2) using EG (3) as an entrainer (lines, predicted values by the UNIFAC model; scattered points, experimental data; ×, $x_3 = 0$; □, $x_3 = 20\%$; ○, $x_3 = 30\%$; △, $x_3 = 40\%$).

nonpolar surface region (-0.0082 e/Å$^2 < \sigma < 0.0082$ e/Å^2), hydrogen bond donor region ($\sigma < -0.0082$ e/Å^2), and hydrogen bond acceptor region ($\sigma > 0.0082$ e/Å^2) [45,46]. As shown in Fig. 6(a), most of the σ-profiles of methylal are within nonpolar surface region, and only a small part is in the hydrogen bond acceptor region, thus indicating that methylal is a week hydrogen bond acceptor. However, the σ-profiles of methanol and EG cover a wide range, and a large part of each is in the hydrogen bond donor and acceptor regions, indicating that methanol and EG are either strong hydrogen bond acceptors or strong hydrogen bond donors. As shown in Fig. 6(b), the strongly negative σ-potentials of methanol and EG in the hydrogen bond donor and acceptor regions indicate that methanol and EG have a strong affinity toward other hydrogen bond donor or acceptor molecules. Methanol and EG have similar properties, thus forming strong hydrogen bonds between them. Thus, the relative volatility of methylal to methanol can be improved by the strong hydrogen bonds between methanol and EG.

4.5. Process simulation & design

4.5.1. Flow sheet

The separation process for the methylal and methanol mixture (95 wt% methylal + 5 wt% methanol) with EG as an entrainer was simulated using the Aspen Plus software (version 8.4) with the rigorous EQ stage model RadFrac. Fig. 7 shows the flow sheet of the extractive distillation process, which is composed of an extractive distillation column (EDC) and a solvent recovery column (SRC). The mixed methylal and methanol are fed into the middle stage of the EDC, while the entrainer is introduced from the top of the EDC.

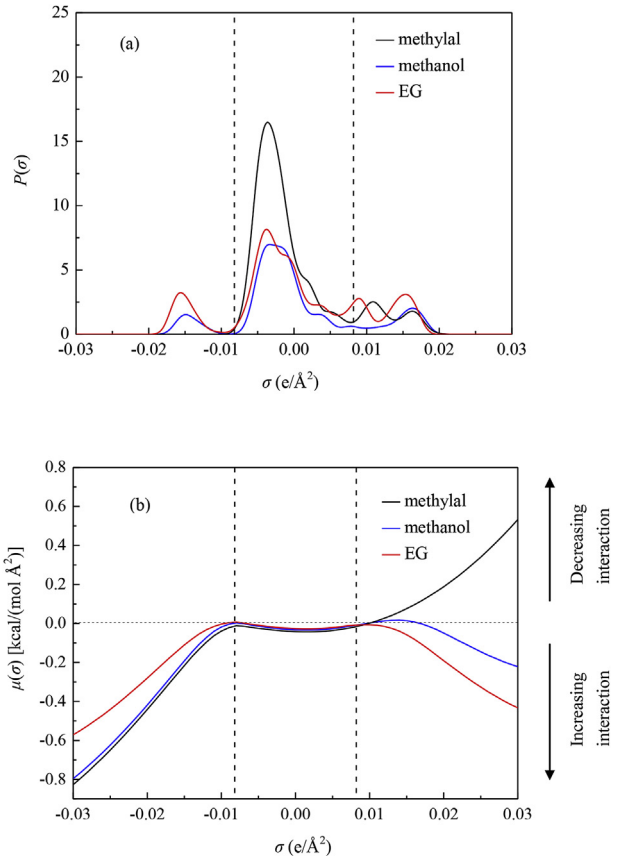

Fig. 6. σ-Profiles of methylal, methanol, and EG (a) and σ-potentials of methylal, methanol, and EG (b).

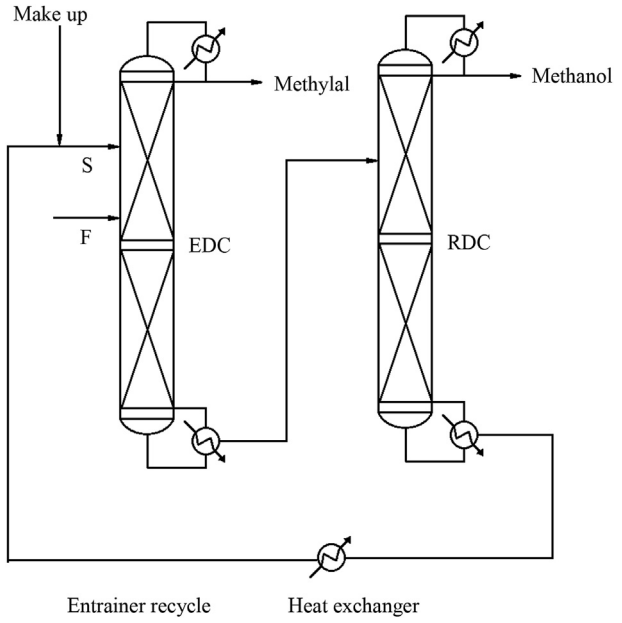

Fig. 7. Process flowsheet for the separation of methylal and methanol by extractive distillation (F, feed stream; S, entrainer stream).

Methylal is obtained at the top of the EDC, and the mixed entrainer and methanol are obtained at the bottom. In the SRC, the entrainer and methanol are separated from the bottom and top, respectively,

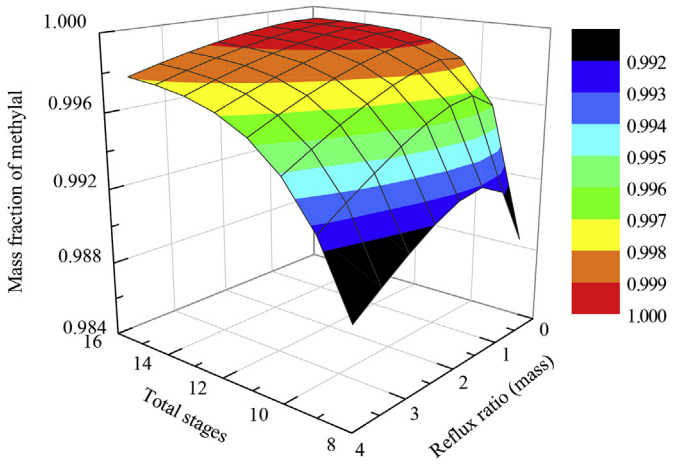

Fig. 8. Influence of the reflux ratio and number of total stages of the EDC on the mass fraction of methylal in the product. Operational conditions: F feed stage is 7, S feed stage is 3, and S/F ratio is 1.0.

because of the large difference between their boiling points. Then, the entrainer at the bottom of the SRC is recycled back into the top of EDC after being cooled. A fresh EG stream is used to replenish the minor loss of EG in the EDC.

The constraints for the optimized specifications are: (1) the mass purity of methylal at the top of the EDC must be more than 99.9%; (2) the mass purity of methanol at the top of the SRC must be more than 95%; and (3) the mass purity of the entrainer at the bottom of the SRC must be more than 99.9%.

4.5.2. Sensitivity analysis

The operating conditions of the extractive distillation process were determined by sensitivity analysis. The following operating parameters are concerned: the number of total stages of EDC and SRC, the reflux ratios of EDC and SRC, the mass ratio of the entrainer to the feed (S/F) of EDC, the mixture (F) feed stage and the entrainer (S) feed stage of EDC, and the feed stage of SRC.

The influence of the reflux ratio and number of total stages of EDC on the mass fraction of methylal in the product is shown in Fig. 8. In some regions, the methylal purity decreases as the reflux ration increases because EG in the liquid phase is diluted by the high reflux ratio. Moreover, when stage number is more than 11 and the reflux ratio is in the range of 0.5–1.5, 99.9 wt% methylal can be obtained.

The influence of the reflux ratio and mass ratio of S/F in the EDC on the mass fraction of methylal in the product is shown in Fig. 9. For the given separation system, the separation objective can be attained when S/F exceeds a limited value (0.9). However, more energy consumption is required for higher S/F and reflux ratio. Thus, the minimum S/F (0.9) and reflux ratio (0.6) were selected to ensure the product purity requirement.

The influence of the mixture feed stage and the entrainer feed stage on the mass fraction of methylal in the product is shown in Fig. 10. The entrainer feed near the top of the EDC is favorable for the separation; this is attributed to the long contact time between the methylal-methanol mixture and EG. When the entrainer feed stage is too close to the top of the EDC, a small amount of the entrainer will volatilize into the top product. Therefore, the third stage is chosen for the S feed stage. In addition, the purity of methylal reaches a maximum value when the F feed stage is 7. Therefore, the F and S feed stages are set to 7 and 3, respectively.

The influence of the reflux ratio and number of total stages of the SRC on the mass fraction of EG is shown in Fig. 11. The

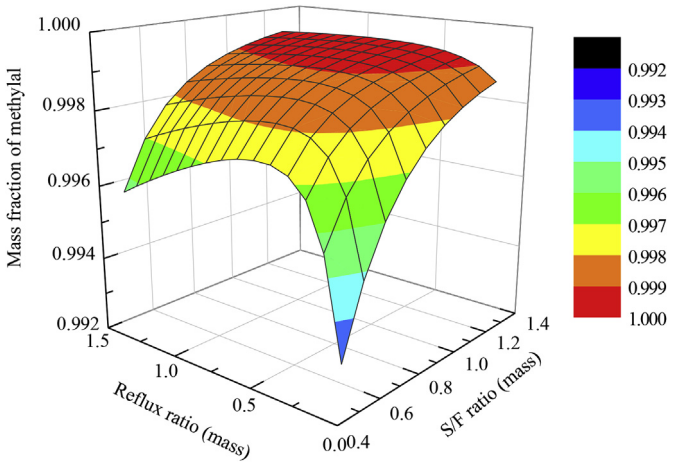

Fig. 9. Influence of the reflux ratio and mass ratio of S/F in the EDC on the mass fraction of methylal in the product. Operational conditions: F feed stage is 7, S feed stage is 3, and the number of total stages of EDC is 11.

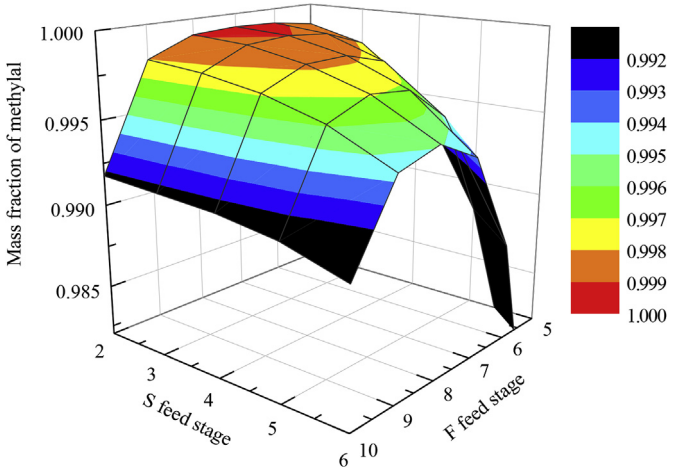

Fig. 10. Influence of the mixture feed stage and the entrainer feed stage on the mass fraction of methylal in the product. Operational conditions: S/F ratio is 0.9, reflux ratio is 0.6, and the number of total stages of EDC is 11.

separation objective can be attained with only 4 stages because of the large difference between the boiling points of methanol and EG. Moreover, at a higher reflux ratio, a higher purity of EG can be obtained and more energy consumption is required. To reduce the operating cost, the proper reflux ratio is in the range of 3–5 with 4 column stages.

The influence of the reflux ratio and the feed stage of SRC on the mass fraction of EG is shown in Fig. 12. When the feed stage is 3 in a 4-stage column, the separation objective can be attained, provided that the reflux ratio exceeds a limited value. To obtain 99.9 wt% EG, the minimum reflux ratio (3.8) was selected.

4.5.3. Simulation results

The simulation results showed that 99.9 wt% methylal can be obtained at the top of the EDC, while 96.4 wt% methanol and 99.9 wt% EG can be obtained at the top and bottom of the SRC, respectively. For more details, please see Tables 7 and 8.

The liquid and vapor molar composition profiles of methylal, methanol, and EG along the EDC are shown in Fig. 13. The condenser and the reboiler are stages 1 and 11, respectively. Two abrupt changes exist for the liquid molar fractions of methylal and

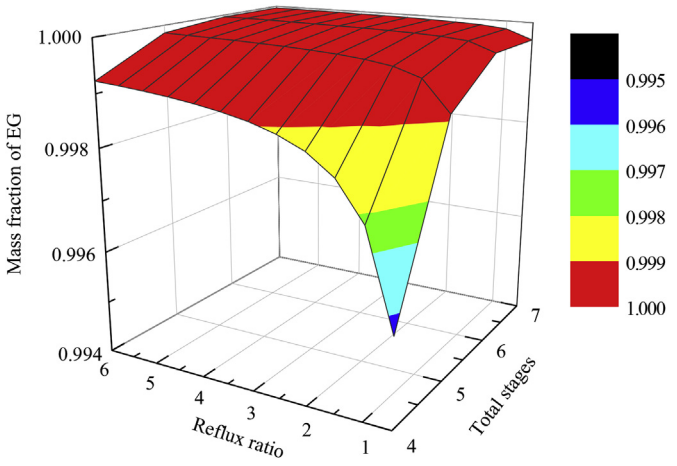

Fig. 11. Influence of the reflux ratio and number of total stages of SRC on the mass fraction of EG. Operational conditions: feed stage is 3.

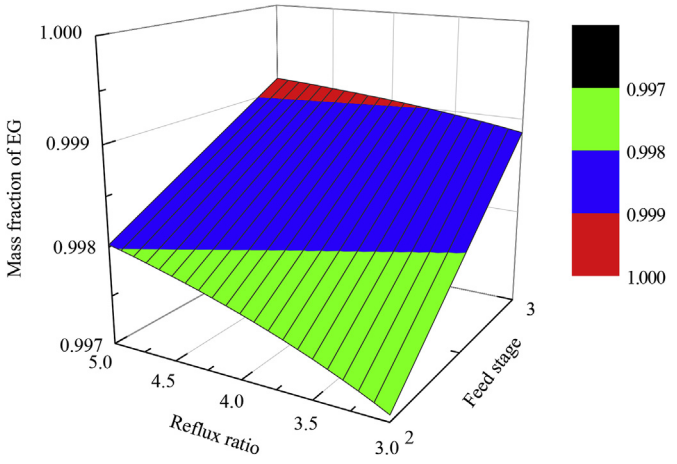

Fig. 12. Influence of the reflux ratio and the feed stage of SRC on the mass fraction of EG. Operational conditions: the total number of stages of the SRC is 4.

Table 7
Optimized specifications and operating conditions for the separation of methylal and methanol using EG as an entrainer.

Contents		
Columns	Extractive distillation column (EDC)	
	Pressure (atm)	1
	Total stages	11
	Feed stage	7
	Entrainer feed stage	3
	Mass reflux ratio	0.6
	Distillate rate (kg/h)	95
	Solvent recovery column (SRC)	
	Pressure (atm)	1
	Total stages	4
	Feed stage	3
	Mass reflux ratio	3.8
	Bottom rate (kg/h)	90
Streams	Feed stream	
	Temperature (°C)	25
	Pressure (atm)	1
	Component flow rate (kg/h)	
	Methylal	95
	Methanol	5
	Entrainer stream	
	Temperature (°C)	25
	Pressure (atm)	1
	Component flow rate (kg/h)	
	EG	90

Table 8
Process simulation results using the EQ stage model.

Contents			
Streams	Top stream of EDC	Temperature (°C)	41.92
		Methylal product purity (mass fraction)	0.999
	Bottom stream of EDC	Temperature (°C)	129.38
		Composition (mass fraction)	
		Methylal	0.001
		Methanol	0.052
		EG	0.947
	Top stream of SRC	Temperature (°C)	63.80
		Methanol content (mass fraction)	0.964
	Recycled entrainer stream	Temperature (°C)	194.84
		Composition (mass faction)	
		Methanol	0.001
		EG	0.999
Heat duty	EDC	Condenser (kW)	−15.68
		Reboiler (kW)	23.55
	SRC	Condenser (kW)	−7.52
		Reboiler (kW)	11.87
	Total heat duty	Reboiler (kW)	35.42
	Heat exchanger (HEAT)	Inlet temperature (°C)	194.84
		Outlet temperature (°C)	25
		Heat duty (kW)	−11.25

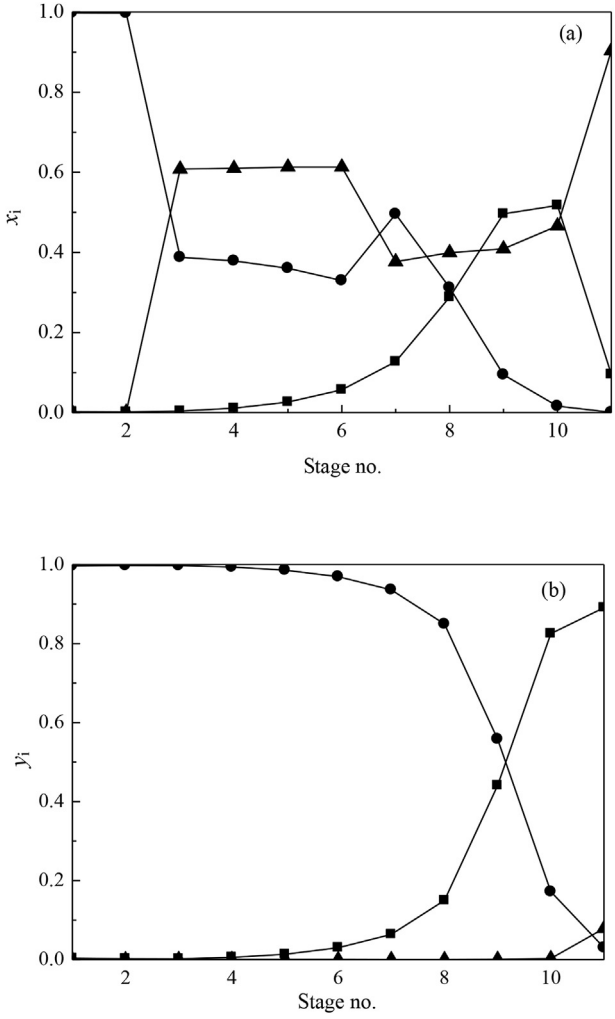

Fig. 13. The liquid and vapor molar composition profiles of methylal, methanol, and EG along the EDC. (a, mole fraction in the liquid phase; b, mole fraction in the vapor phase; ●, methylal; ■, methanol; ▲, EG; the stages are numbered from the top to bottom).

EG because of EG and the methylal-methanol mixture feed at stages 3 and 7, respectively (see Fig. 13(a)). Moreover, the methylal composition decreases from the top to bottom, and essentially only methanol and EG are present at the bottom. The content of EG in the vapor phase is very low because of its high boiling point (see Fig. 13(b)).

5. Conclusions

In this work, the separation of methylal and methanol by extractive distillation was intensified using EG as an entrainer. The predictions for a suitable entrainer using the COSMO-RS model and the VLE experiments for the methylal + methanol + EG ternary system showed that the relative volatility of methylal to methanol is significantly improved using EG as an entrainer, indicating that EG is a suitable entrainer.

Furthermore, the σ-profiles and σ-potentials obtained using the COSMO-RS model provide theoretical insights into the separation mechanism at a molecular level. Methanol and EG are either strong hydrogen bond acceptors or strong hydrogen bond donors, thus easily forming a hydrogen bond between methanol and EG, improving the relative volatility of methylal to methanol.

Based on the VLE data, the UNIFAC model was extended to the methylal–methanol–EG system. Then, a simulation of the extractive distillation process for the separation of methylal and methanol with the obtained UNIFAC model parameters was conducted with the EQ stage model. The proper operating conditions were obtained by sensitivity analysis. The simulation results showed that EG is an effective and efficient entrainer to separate the methylal and methanol mixture.

Acknowledgements

This work is financially supported by the National Natural Science Foundation of China under Grants (Nos. 21476009, 21406007, and U1462104).

References

[1] L. Berg, Separation of benzene and toluene from close boiling nonaromatics by extractive distillation, AIChE J. 29 (2010) 961–966.
[2] M.J. Earle, J.M. Esperança, M.A. Gilea, J.N. Lopes, L.P. Rebelo, J.W. Magee, K.R. Seddon, J.A. Widegren, The distillation and volatility of ionic liquids,

Nature 439 (2006) 831–834.
[3] P. Langston, N. Hilal, S. Shingfield, S. Webb, Simulation and optimisation of extractive distillation with water as solvent, Chem. Eng. Process. Process Intensif 44 (2005) 345–351.
[4] J. Qin, Q. Ye, X. Xiong, N. Li, Control of benzene–cyclohexane separation system via extractive distillation using sulfolane as entrainer, Ind. Eng. Chem. Res. 52 (2013) 10754–10766.
[5] E. Carretier, P. Moulin, M. Beaujean, F. Charbit, Purification and dehydration of methylal by pervaporation, J. Membr. Sci. 217 (2003) 159–171.
[6] J. Burger, M. Siegert, E. Ströfer, H. Hasse, Poly(oxymethylene) dimethyl ethers as components of tailored diesel fuel: properties, synthesis and purification concepts, Fuel 89 (2010) 3315–3319.
[7] Y. Ren, Z.H. Huang, D.M. Jiang, L.X. Liu, K. Zeng, B. Liu, X.B. Wang, Engine performance and emission characteristics of a compression ignition engine fuelled with diesel/dimethoxymethane blends, Proc. Inst. Mech. Eng. Part D 219 (2005) 905–914.
[8] J.O. Weidert, J. Burger, M. Renner, S. Blagov, H. Hasse, Development of an integrated reaction–distillation process for the production of methylal, Ind. Eng. Chem. Res. 56 (2017) 575–582.
[9] E. Lladosa, J.B. Montón, M.C. Burguet, R. Muñoz, Phase equilibria involved in extractive distillation of dipropyl ether + 1-propyl alcohol using 2-ethoxyethanol as entrainer, Fluid Phase Equil. 255 (2007) 62–69.
[10] Z. Lei, R. Zhou, Z. Duan, Process improvement on separating C4 by extractive distillation, Chem. Eng. J. 85 (2002) 379–386.
[11] Z. Lei, R. Zhou, Z. Duan, Application of scaled particle theory in extractive distillation with salt, Fluid Phase Equil. 200 (2002) 187–201.
[12] M. Seiler, C. Jork, A. Kavarnou, W. Arlt, R. Hirsch, Separation of azeotropic mixtures using hyperbranched polymers or ionic liquids, AIChE J. 50 (2004) 2439–2454.
[13] X. Sun, H. Luo, S. Dai, Ionic liquids-based extraction: a promising strategy for the advanced nuclear fuel cycle, Chem. Rev. 112 (2012) 2100–2128.
[14] H. Liu, H. Gao, Y. Ma, Z. Gao, W. Eli, Synthesis of high-purity methylal via extractive catalytic distillation, Chem. Eng. Technol. 35 (2012) 841–846.
[15] Q. Wang, B. Yu, C. Xu, Design and control of distillation system for methylal/methanol separation. Part 1: extractive distillation using DMF as an entrainer, Ind. Eng. Chem. Res. 51 (2012) 1281–1292.
[16] M.A.S.S. Ravagnani, M.H.M. Reis, R.M. Filho, M.R. Wolf-Maciel, Anhydrous ethanol production by extractive distillation: a solvent case study, Process Saf. Environ. Protect. 88 (2010) 67–73.
[17] G.J.A.F. Fien, Y.A. Liu, Heuristic synthesis and shortcut design of separation processes using residue curve maps: a review, Ind. Eng. Chem. Res. 33 (1994) 2505–2522.
[18] V.N. Kiva, E.K. Hilmen, S. Skogestad, Azeotropic phase equilibrium diagrams: a survey, Chem. Eng. Sci. 58 (2003) 1903–1953.
[19] M.F. Doherty, G.A. Caldarola, Design and synthesis of homogeneous azeotropic distillations. 3. The sequencing of columns for azeotropic and extractive distillations, Ind. Eng. Chem. Fundam. 24 (1985) 474–485.
[20] Q. Li, J. Zhang, Z. Lei, J. Zhu, J. Zhu, X. Huang, Selection of ionic liquids as entrainers for the separation of ethyl acetate and ethanol, Ind. Eng. Chem. Res. 48 (2009) 9006–9012.
[21] Q. Li, F. Xing, Z. Lei, B. Wang, Q. Chang, Isobaric vapor–liquid equilibrium for isopropanol + water + 1-Ethyl-3-methylimidazolium tetrafluoroborate, Petrochem. Technol. 53 (2008) 275–279.
[22] Q. Li, J. Zhang, Z. Lei, J. Zhu, F. Xing, Isobaric Vapor–Liquid equilibrium for ethyl acetate + ethanol + 1-Ethyl-3-methylimidazolium tetrafluoroborate, J. Chem. Eng. Data 54 (2009) 193–197.
[23] C. Kuhnert, M. Albert, S. Breyer, I. Hahnenstein, H. Hasse, G. Maurer, Phase equilibrium in formaldehyde containing multicomponent mixtures: experimental results for fluid phase equilibria of (formaldehyde + (water or methanol) + methylal)) and (formaldehyde + water + methanol + methylal) and comparison with predictions, Ind. Eng. Chem. Res. 45 (2006) 5155–5164.
[24] H.K. Hansen, P. Rasmussen, A. Fredenslund, M. Schiller, J. Gmehling, Vapor-liquid equilibria by UNIFAC group contribution. 5. Revision and extension, Ind. Eng. Chem. Res. 30 (1991) 2352–2355.
[25] M. Albert, I. Hahnenstein, H. Hasse, G. Maurer, Vapor–Liquid and Liquid–Liquid equilibria in binary and ternary mixtures of water, methanol, and methylal, J. Chem. Eng. Data 46 (2001) 897–903.
[26] 1,2-Ethanediol, (n.d.). http://webbook.nist.gov/cgi/cbook.cgi?ID=C107211&Units=SI&Mask=4#Thermo-Phase (accessed December 16, 2017).
[27] A. Klamt, Conductor-like screening model for real solvents: a new approach to the quantitative calculation of solvation phenomena, J. Phys. Chem. 99 (1995) 2224–2235.
[28] A. Klamt, F. Eckert, COSMO-RS: a novel and efficient method for the a priori prediction of thermophysical data of liquids, Fluid Phase Equil. 172 (2000) 43–72.
[29] J. Zhang, D. Peng, Z. Song, T. Zhou, H. Cheng, L. Chen, Z. Qi, COSMO-descriptor based computer-aided ionic liquid design for separation processes. Part I: modified group contribution methodology for predicting surface charge density profile of ionic liquids, Chem. Eng. Sci. 162 (2017) 355–363.
[30] H. Grensemann, J. Gmehling, Performance of a conductor-like screening model for real solvents model in comparison to classical group contribution methods, Ind. Eng. Chem. Res. 44 (2005) 1610–1624.
[31] T. Banerjee, A. Khanna, Infinite dilution activity coefficients for trihexyltetradecyl phosphonium ionic liquids: measurements and COSMO-RS prediction, J. Chem. Eng. Data 51 (2006) 2170–2177.
[32] M. Diedenhofen, A. Klamt, COSMO-RS as a tool for property prediction of IL mixtures—a review, Fluid Phase Equil. 294 (2010) 31–38.
[33] A. Klamt, V. Jonas, A. Thorsten Bürger, J.C.W. Lohrenz, Refinement and parametrization of COSMO-RS, J. Phys. Chem. A 102 (1998) 5074–5085.
[34] F. Eckert, A. Klamt, Fast solvent screening via quantum chemistry: COSMO-RS approach, AIChE J. 48 (2002) 369–385.
[35] A.V. Orchillés, P.J. Miguel, V. Gonzálezalfaro, E. Vercher, A. Martínezandreu, Isobaric vapor–liquid equilibria of 1-propanol + water + trifluoromethanesulfonate-based ionic liquid ternary systems at 100 kPa, J. Chem. Eng. Data 56 (2011) 4454–4460.
[36] Q. Li, W. Zhu, Y. Fu, H. Wang, L. Li, B. Wang, Isobaric vapor–liquid equilibrium for methanol + dimethyl carbonate + 1-Octyl-3-methylimidazolium tetrafluoroborate, J. Chem. Eng. Data 57 (2012) 1602–1606.
[37] E. Quijada-Maldonado, G.W. Meindersma, A.B.D. Haan, Ionic liquid effects on mass transfer efficiency in extractive distillation of water–ethanol mixtures, Comput. Chem. Eng. 71 (2014) 210–219.
[38] M.T.G. Jongmans, E. Hermens, M. Raijmakers, J.I.W. Maassen, B. Schuur, A.B.D. Haan, Conceptual process design of extractive distillation processes for ethylbenzene/styrene separation, Chem. Eng. Res. Des. 90 (2012) 2086–2100.
[39] J.J. Figueroa, B.H. Lunelli, R.M. Filho, M.R.W. Maciel, Improvements on anhydrous ethanol production by extractive distillation using ionic liquid as solvent, Procedia Eng 42 (2012) 1016–1026.
[40] W.B. Ramos, M.F. Figueiredo, R.P. Brito, Optimization of extractive distillation process with a single column for anhydrous ethanol production, Comput. Aided Chem. Eng 33 (2014) 1411–1416.
[41] L. Laroche, H.W. Andersen, M. Morari, N. Bekiaris, Homogeneous azeotropic distillation: comparing entrainers, Can. J. Chem. Eng. 70 (2010) 1302–1319.
[42] J. Wisniak, The Herington test for thermodynamic consistency, Ind. Eng. Chem. Res. 33 (1994) 177–180.
[43] G. Yu, C. Dai, L. Wu, Z. Lei, Natural gas dehydration with ionic liquids, Energy Fuels 31 (2017) 1429–1439.
[44] D. Peng, J. Zhang, H. Cheng, L. Chen, Z. Qi, Computer-aided ionic liquid design for separation processes based on group contribution method and COSMO-SAC model, Chem. Eng. Sci. 159 (2017) 58–68.
[45] J. Li, X. Yang, K. Chen, Y. Zheng, C. Peng, H. Liu, Sifting ionic liquids as additives for separation of acetonitrile and water azeotropic mixture using the COSMO-RS method, Ind. Eng. Chem. Res. 51 (2012) 9376–9385.
[46] T. Banerjee, M.K. Singh, A. Khanna, Prediction of binary VLE for imidazolium based ionic liquid systems using COSMO-RS, Ind. Eng. Chem. Res. 45 (2006) 3207–3219.